

Effects of sorbed water on crack propagation in poly(methyl methacrylate) under static tensile stress

Y. BOKOI, C. ISHIYAMA, M. SHIMOJO

Precision and Intelligence Laboratory, Tokyo Institute of Technology, 4259 Nagatsuta, Midori-ku, Yokohama, 226, Japan
E-mail: cishiyam@pi.titech.ac.jp

Y. SHIRAISHI

Mitsubishi Engineering Plastics Corporation, 5-6-2, Higashiyawata, Hiratsuka, 254, Japan

Y. HIGO

Precision and Intelligence Laboratory, Tokyo Institute of Technology, 4259 Nagatsuta, Midori-ku, Yokohama, 226, Japan

Effects of sorbed water on crack propagation in poly(methyl methacrylate) (PMMA) under static tensile stress have been investigated. The specimens were kept for more than two years in temperature and humidity-controlled conditions. Sorbed water of less than 0.40 wt% scarcely affected K_{th} value (threshold stress intensity factor for crack propagation), however, K_{th} value for the specimens containing water of more than 0.40 wt% increased with the amount of sorbed water. K_{th} values related to the balance among the radius of the curvature of crack tip, crazing stress and craze fibril rupture stress, which are functions of the amount of sorbed water. At a crack propagation rate of more than 1×10^{-7} m/s, the slopes of K - da/dt curves for the specimens containing water less than 0.40 wt% were gentle, however, that for the specimens containing more than 0.40 wt% was steep; and unstably fractured. It was found that the gentler slopes for the specimens containing little sorbed water may be caused by craze-shear controlled crack propagation mechanisms, while the steeper slopes for the other specimens may be caused by a craze controlled crack propagation mechanism. © 2000 Kluwer Academic Publishers

1. Introduction

Generally, the crack propagation behavior of materials is strongly affected by the plastic deformation behavior near the crack tip. For polymers, it has been observed that the plastic zone consists of a single craze [1–5], multiple crazes [6–8], shear bands [9], a combination of them [10,11] or homogeneous deformation [12]; for example, the plastic zone near the crack tip in high-molecular-weight PMMA was reported to consist of a single craze [1–5]. Crack propagation behavior of various polymers has been investigated, however, it seems that the studies have not reached application to damage tolerant design of materials, because the factors to determine crack propagation threshold and crack propagation rate, which are significant aspects of crack propagation behavior, have not been clarified. One of the reasons why the factors are not determined is that the amount of sorbed water in the materials is not sufficiently adjusted. Sorbed water acts as a plasticizer, reduces crazing stress and enhances craze growth and fracture toughness for PMMA [13–17]. This suggests that crack propagation behavior of polymers should depend on sorbed water.

In this paper, we studied the effects of sorbed water on the crack propagation behavior, that is, crack propagation threshold and crack propagation rate of a non-crystalline polymer, PMMA, under static loading in temperature-humidity controlled environments, and the relationship among the amount of sorbed water, crazing behavior and crack propagation behavior are discussed. Crack propagation under static loading is termed CPS in this paper. Crazing behavior, which depends on the amount of sorbed water, is investigated under creep test.

2. Experimental procedure

2.1. Materials

Two cast sheets of PMMA which had been made as commercial grade, Acrylite (made by Mitsubishi Rayon Co., Ltd.) were used. The thicknesses of the sheets were 20 mm and 1 mm, respectively. The weight-average molecular weight (M_w) and the number-average molecular weight (M_n), determined by gel permeation chromatography analysis, were $M_w = 4,000,000$ and $M_n = 1,430,000$, respectively.

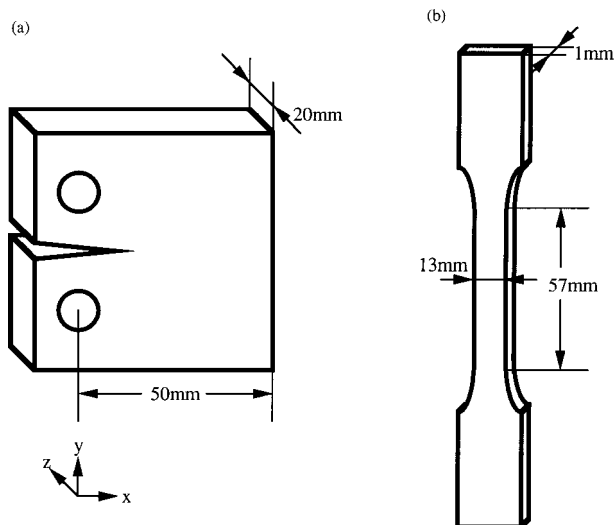


Figure 1 Drawing of CT specimen and creep specimen. (a) CT specimen. The x , y and z directions are defined for the specimen. (b) Creep specimen. This shape is on ASTM tensile specimen.

CPS tests were carried out using CT specimens ($W = 50$ mm, $B = 20$ mm) machined from the sheet of a thickness of 20 mm, while creep tests to observe crazing behavior were carried out using unnotched creep test specimens (gauge length = 57 mm, gauge width = 13 mm, thickness = 1 mm) machined from the sheet of a thickness of 1 mm. The dimensions of the both specimens are shown in Fig. 1. The x , y and z directions for CT specimens are defined as shown in Fig. 1a.

All specimens were carefully cleaned in pure water using an ultrasonic washer, then were annealed at a temperature of 90 °C for 12 hours to remove any residual stress. Each specimen had been stored at a temperature of 20 °C and a humidity of either 12, 34, 55, 75 or 97%RH (relative humidity) for more than 2 years to adjust the amount of sorbed water and to disperse sorbed water in specimens as homogeneously as possible. The humidity was controlled with a saturated salt solution which produced constant humidity. Water content (C) in the samples was obtained as follows;

$$C = \frac{W_f - W_i}{W_i} \times 100 \text{ (wt\%)} \quad (1)$$

where C is water content, W_i is the weight of a sample after annealing and W_f is the weight of the sample containing sorbed water. The water content of each CT specimen increases with time passing (Fig. 2). It can be estimated that sorbed water becomes in equilibrium with each environmental humidity after 15,000 hours. Sorbed water in creep test specimens can become in equilibrium with each environmental humidity in shorter time than that in CT specimens, because creep test specimens is thinner than CT specimens. Each sample in sorption equilibrium with the environment was employed for the tests. Equilibrated water content shown in Table I is the average value of three samples at each relative humidity.

A strain gauge was pasted on the back side of each CT specimen, to measure the crack length using a compliance method.

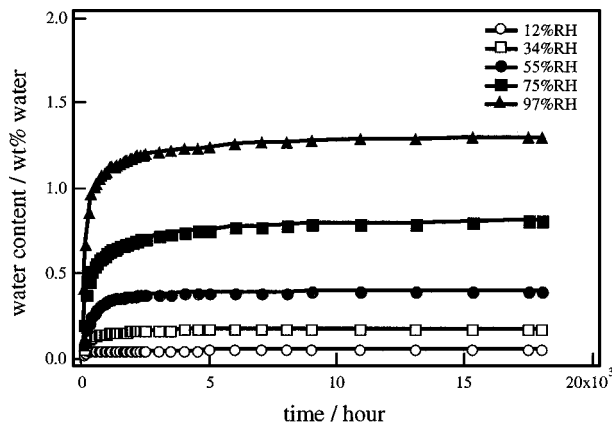


Figure 2 Water content vs. time. Each CT specimen was stored at constant temperature (20 °C) and a relative humidity; 12%RH, 34%RH, 55%RH, 75%RH and 97%RH.

TABLE I Water contents of CT specimens and tensile specimens, which were kept for 2 years

relative humidity /%RH	CT specimen		Tensile specimen	
	water content /wt%	designation	water content /wt%	designation
12	0.05	0.05CT	0.06	0.05CR
34	0.17	0.15CT	0.15	0.15CR
55	0.40	0.40CT	0.38	0.40CR
75	0.81	0.80CT	0.90	0.80CR
97	1.30	1.30CT	1.40	1.30CR

2.2. CPS test

CPS tests were carried out under load control in a tensile mode using a Shimadzu servo hydraulic testing machine. CT specimens which contain 0.05–1.30 wt% water, as shown in Table I, were used. These specimens are designated 0.05CT, 0.17CT, 0.40CT, 0.80CT and 1.30CT, according to their water contents. A pre-crack of 2 mm was introduced under cyclic loading at a stress intensity factor range (ΔK_I) of less than 0.7 MPa \sqrt{m} . Then, uniaxial constant load was applied to each CT specimen in mode I. The crack length was measured using both a compliance method and a direct measuring method using a travelling microscope. Both the applied load and the back strain were recorded with a data logger at regular intervals. CPS tests were carried out in a test cell, the inside of which was kept at a given constant relative humidity. Relative humidity was controlled by an accurate humidity generator, which provided a mixture of dry and wet air at a given rate. Temperature during the tests was kept at 37 °C, because the effects of sorbed water on plasticization at 37 °C would appear more remarkably than that at 20 °C. A temperature and humidity tracer was used to monitor the environmental condition in the test cell. After CPS tests, fracture surfaces of specimens were observed using both of a confocal scanning laser microscope, by which the roughness of the fracture surface could be measured, and an optical microscope. The roughness was defined as the difference in height between the lowest point and the highest point on a region which was displayed by the laser microscope.

2.3. Creep test

Creep tests were carried out in a test cell, the inside of which was kept at a temperature of 37 °C at a given constant relative humidity. Creep test specimens which contained 0.06–1.40 wt% water, as shown in Table I, were designated 0.05CR, 0.15CR, 0.40CR, 0.80CR, 1.30CR, according to their water contents. Two kinds of tests were carried out. One is to measure crazing stress and creep rupture stress when a constant stress was applied. In the other tests, after a constant stress was applied to creep test specimens for a period of time and released, surfaces of specimens were observed using an optical microscope and the geometry of surface crazes on the tested specimens was measured using a digitizer.

3. Results

3.1. CPS tests

Fig. 3 shows logarithmic plots of crack propagation rate per second (da/dt) vs. stress intensity factor (K_I) for samples containing various amounts of sorbed water. It can be seen from Fig. 3 that the amount of sorbed water complicatedly changes the CPS behavior of PMMA.

The stress intensity factor at crack propagation rate of less than 1×10^{-8} m/s is defined as K_{Ith} in this paper. It is obviously seen that sorbed water in CT specimens controls K_{Ith} values. The K_{Ith} values for three samples containing water of less than 0.40 wt% are 0.86 to 0.89 $\text{MPa}\sqrt{\text{m}}$ and closely similar values with one another are obtained, while the K_{Ith} values for three samples containing water more than 0.40 wt% increase with water content. This shows that sorbed water of more than 0.40 wt% has strong effect on the increase in K_{Ith} .

The K_{Ith} values for 0.05CT and 0.15CT are nearly equal to that for 0.40CT, however, the slopes of CPS curves for the formers are gentler than that for the latter

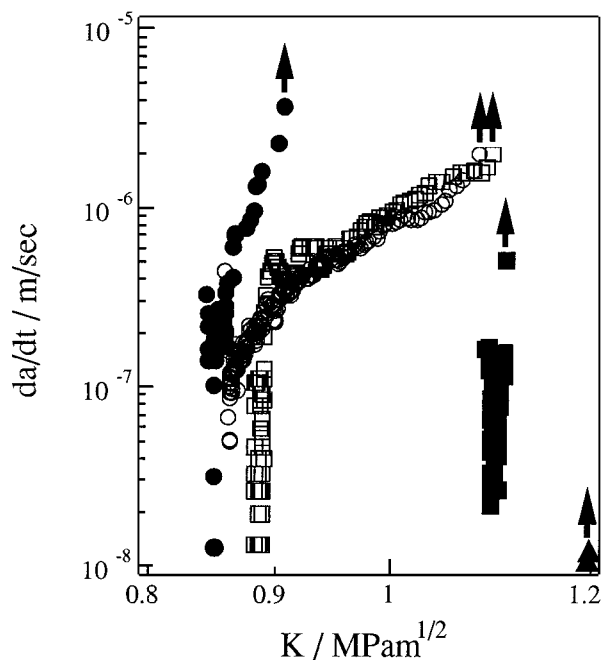


Figure 3 Crack propagation rates vs. stress intensity factor. 0.05CT(○), 0.15CT(□), 0.40CT(●), 0.80CT(■) and 1.30CT(▲). Arrows show unstable fracture.

at a crack propagation rate of more than 1×10^{-7} m/s. This result suggests that crack propagation mechanisms may differ between 0.05CT (or 0.15CT) and 0.40CT. As soon as K_I values for 0.80CT and 1.30CT become higher than that K_{Ith} values (i.e., cracks in these specimens propagate at a crack propagation rate of slightly more than 1×10^{-8} m/s), the crack propagation rates drastically increase. 1.30CT unstably fractures as soon as the crack starts to propagate, despite the K_{Ith} value is higher than those obtained in the other CT specimens tested.

3.2. Creep tests

3.2.1. Crazing stress and creep rupture stress

Fig. 4a is presented as the logarithm of stress versus the logarithm of rupture life time. The rupture life time decreases with an increase in the amount of sorbed water. Fig. 4b shows creep rupture stress as a function of the amount of sorbed water. With an increase in the amount of sorbed water, creep rupture stress decreases. The creep rupture stress for 0.05CR is over 1.3 times higher than that for 1.30CR, when the stresses are applied to the specimens for 100 s.

Fig. 4c shows crazing stress as a function of the amount of sorbed water. Each crazing stress is the stress at which crazes are observed on the creep test specimen tested for a period of 100 s or 1000 s. Crazing stress decreases as an increase in the amount of sorbed water. This trend is similar to that of creep rupture stress, however, the effect of sorbed water more than 0.40 wt% on crazing stress is only a little. Creep rupture stress and crazing stress are compared in Fig. 4d. The creep rupture stress curves shown in Fig. 4c are the same as those in Fig. 4b, and the crazing stress curve is the result tested for a period of 100 s. When a stress of 56 MPa is applied to 0.05CR, crazes are observed in 100 s and the sample ruptures in 5000 s. When a stress of 46 MPa is applied to 1.30CR, crazes are observed in 100 s and the sample ruptures in less than 1000 s. The interval between craze appearance and creep rupture for 0.05CR is much longer than that for 1.30CR. The intervals for 0.15CR and 0.40CR are also longer than that for 1.30CR. This shows that the intervals decreases with an increase in amount of sorbed water, when amount of sorbed water is more than 0.40 wt%.

If craze fractures when creep rupture stress is applied to craze, it is presumed that K_{Ith} would decrease and crack propagation rate would increase with an increase in amount of sorbed water. However, in CPS test, the K_{Ith} for 1.30CT is much higher than those for the other samples. This suggests that CPS behavior may depend on some other factors.

3.2.2. Craze geometry

Figs 5a–c show micrographs of crazes which appear on surfaces of PMMA samples tested under constant stresses for 10,000 s. Crazes which appear on 0.15CR is similar to that of 0.05CR and that of 0.80CR is similar to that of 1.30CR. A number of crazes, the length of which is less than 100 μm , can be seen on 0.05CR

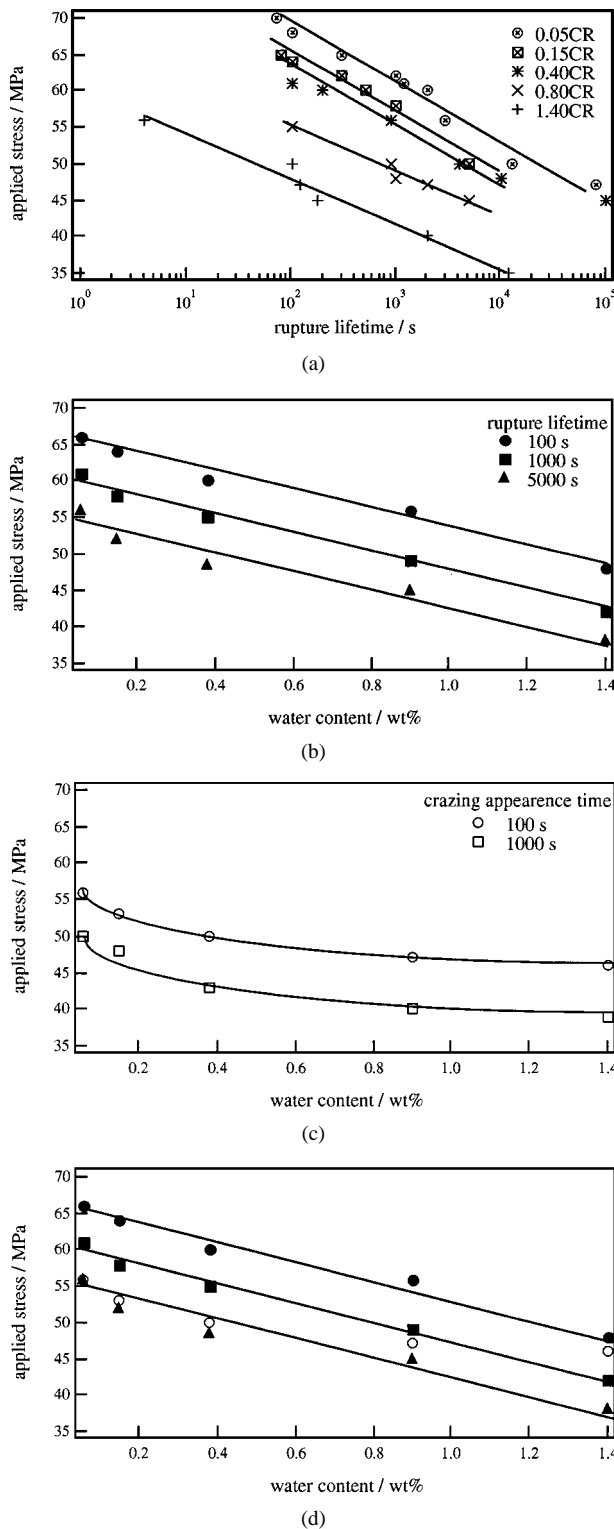


Figure 4 (a) Logarithm of applied stress vs. rupture life time for creep test specimens. (b) Applied stress vs. water content. The parameter is rupture lifetime. The plots are picked up from fitting lines in Fig. 4a. (c) Applied stress at which appear crazes vs. water content. The parameter is the minimum value of time at which crazes appear under a given stress. (d) A comparison between creep rupture stress and crazing stress in 100 s as a function of water content.

and 0.40CR, while a few crazes, the length of which is much more than $100 \mu\text{m}$, can be seen on 1.30CR. These figures qualitatively show that the amount of sorbed water strongly controls craze geometry.

Then, we carried out quantitative analysis of the craze geometry of these samples (0.05CR, 0.40CR and 1.30CR) tested under constant stress.

The average craze length, L_a , is calculated by:

$$L_a = \frac{\sum_{i=1}^n L_i}{n} \quad (2)$$

where L_i is the length of the i -th craze in a surface area of 1 mm^2 on a tested specimen and n is the number of crazes in the surface area. The craze density, ρ , is then given by

$$\rho = \frac{n}{A} \quad (3)$$

where A is the observed surface area. Craze width, w , under various static tensile stresses were also measured.

Fig. 6 shows average craze length as a function of applied time. There is little change in average craze length for each sample with an increase in time. There is also little change in the length with applied stress. The average craze lengths of 0.05CR and 0.40CR remain approximately $10 \mu\text{m}$, and that of 1.30CR remains $100 \mu\text{m}$. These results show that average craze length is independent of both applied stress and time.

Fig. 7 shows that the relationship between craze width and craze length under various stresses. The crazes were randomly selected from all creep specimens tested. Craze width simply increases with craze length. Applying an exponential approximation to the plots, we can obtain a following equation:

$$w = C_0 - C_1 \exp(-C_2 l) \quad (4)$$

$$C_0 = 5.60 \quad / \mu\text{m}$$

$$C_1 = 5.40 \quad / \mu\text{m}$$

$$C_2 = 6.40 * 10^{-2} \quad / 1/\mu\text{m}$$

where w (μm) is craze width and l (μm) is craze length. When we substitute average craze length of each specimen for l in Equation 4, the calculated craze width of 1.30CR is more than twice as great as that of 0.05CR or 0.40CR.

Craze density increases with applied stress (Fig. 8). An increase in craze density of 1.30CR with stress is comparatively a little, while craze density of 0.40CR strongly increases. The craze density of 1.30CR is in an order of 10^7 m^{-2} , while that of 0.40CR is in an order of 10^7 to 10^{10} m^{-2} . As shown in Fig. 9, the craze density of 1.30CR remains comparatively low under a stress of 50 MPa, while those of 0.05CR and 0.40CR increases with time except a slight decrease in craze density just before creep rupture. Craze density decreases with time passing just before the specimens rupture. This is because crazes coalesce and thus n in Equation 3 decreases. Craze appearance time decreases with an increase in amount of sorbed water, because sorbed water may act as a plasticizer.

Table II shows the summary of the creep tests. The crazing stress, creep rupture stress and maximum value of craze density are the data of load applied time of 100 s. It is interesting that the effect of sorbed water as a plasticizer on crazing differ between 0.40CR and 1.30CR. Sorbed water in 0.40CR compels a number of crazes to increase, while that in 1.30CR does the crazes to lengthen.

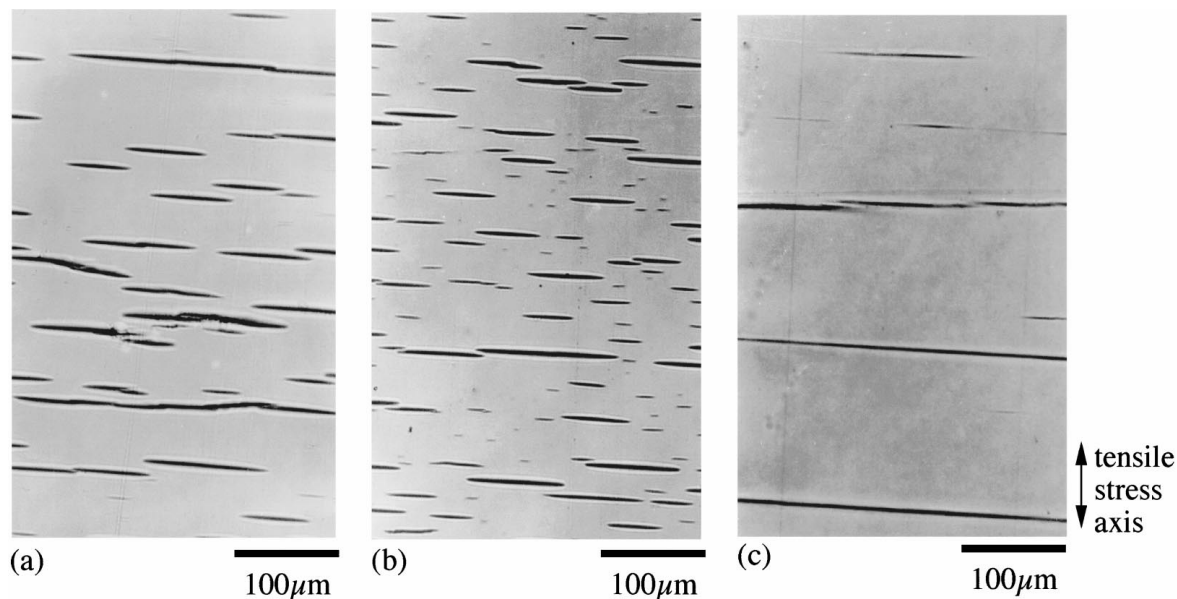


Figure 5 Optical micrographs of surfaces of tensile specimens tested at constant stresses for 10000 sec (a) 0.05CR, and a stress of 50 MPa, (b) 0.40CR, and a stress of 50 MPa, (c) 1.30CR, and a stress of 35 MPa.

TABLE II Summary of creep test

water content/wt% water of creep test specimen (designation)	crazing stress/MPa (applied time 100 sec)	creep rupture stress/MPa (applied time 100 sec)	average craze length/ μm	craze width/ μm	maximum value of craze density/l/m (load applied time 100 sec)
0.06 (0.05CR)	56	66	10	2.5	3.0×10^9
0.38 (0.40CR)	50	62	10	2.7	1.0×10^{10}
1.40 (1.30CR)	46	50	100	5.7	4.0×10^7

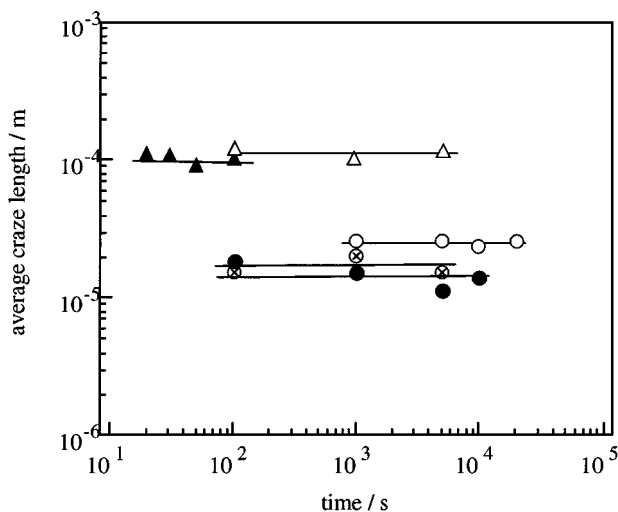


Figure 6 Effects of time on average craze length. 0.05CR at stress of 50 MPa(\circ), 0.05CR at stress of 56 MPa(\otimes), 0.40CR at stress of 50 MPa(\bullet) and 1.30CR at stress of 50 MPa(\blacktriangle) 1.30CR at stress of 46 MPa(\triangle).

4. Discussion

4.1. Effects of sorbed water on K_{Ith} value

As shown in Fig. 3, obviously sorbed water strongly affected K_{Ith} value for each CT specimen, however, it has been unknown what factors to determine K_{Ith} sorbed water affects. In this discussion we attempt to determine the factors to determine K_{Ith} values and to

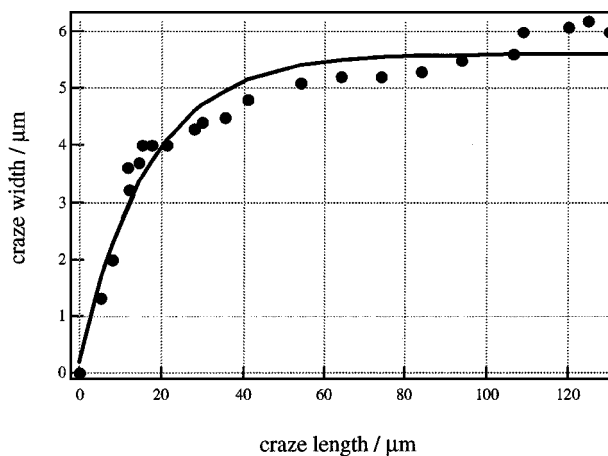


Figure 7 Craze width v.s. craze length. These plots are data of crazes randomly selected in creep specimens tested under a given stress.

clarify the effects of sorbed water on K_{Ith} from the factors.

Fig. 10a–c show micrographs of local regions near crack tips in 0.05CT, 0.40CT and 1.30CT tested under a K_I of $0.8 \text{ MPa}\sqrt{\text{m}}$, which is less than K_{Ith} values for three kinds of CT specimens. When K_I is less than K_{Ith} , no crack propagates and also no crack tip craze grows. The stress which is applied to a local position in the craze under K_{Ith} is a constant stress, which is independent of time. Since it is sure that the craze fibrils orient in a direction of applied loading axis, that is, the y direction as shown in Fig. 1, it is also considered that the

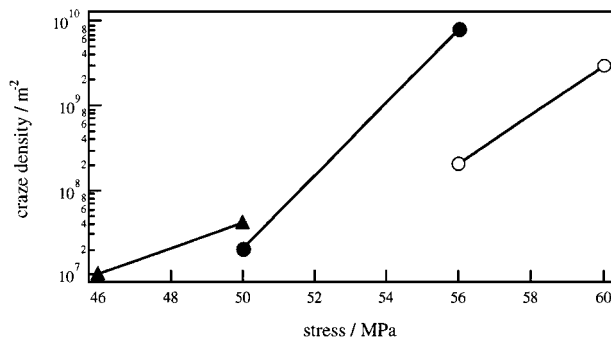


Figure 8 Craze density as a function of applied constant stress for 100 sec. The craze density is numbers of crazes per a unit area. 0.05CR(▲), 0.40CR(●) and 1.30CR(○).

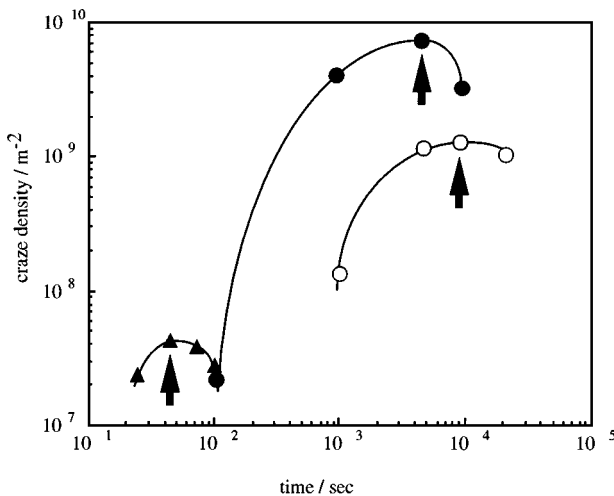


Figure 9 The effect of time on Craze density in PMMA at a constant stress of 50 MPa. 0.05CR(○), 0.40CR(●) and 1.30CR(▲). Each arrow indicates maximum value of craze density on a sample.

stress which is applied to the craze is only tensile stress in the y direction. The stress condition of the crack tip craze becomes equal to that of creep tests except that the stress applied to the crack tip craze may differ among local positions in the craze.

As shown in Fig. 6, craze length was uniform, and it is independent of both applied stress and time. This shows that the difference in stress among local positions in the craze does not affect craze length or craze width as a function of craze length. The craze length and craze width at each crack tip shown in Fig. 10a–c are nearly equal to average craze length and craze width of creep specimen containing the same amount of sorbed water as shown in Table II. These results reinforce validity to apply the results of creep tests to discussion the effects of sorbed water on K_{Ith} . It is assumed that average craze length, craze width and crazing stress which are shown in Table II can be applied to crack tip craze length, craze width and crazing stress, respectively, for CT specimens containing the same amount of sorbed water.

As shown in Fig. 11a and b, the radius of curvature, ρ at a crack tip is a function of width of crack tip crazes and the ρ for 1.30CT is greater than those for the other CT specimens tested. This agrees with result that craze width of 1.30CR is greater than that of 0.05CR or 0.40CR. Craze width of creep test specimens tested increased with a decrease in crazing stress, as shown in

Table II. Thus, with a decrease in crazing stress, the ρ at a crack tip increases. When plastic deformation occurs near a crack tip in a material under mode I, the crack tip becomes blunt. The ρ at the crack tip increases with the crack tip blunting, and as a result, the stress applied to the crack tip is reduced. The maximum value of stress in the y direction on the x axis, $(\sigma_y)_{max}$, decreases with an increase in the ρ at the crack tip, according to elastic fracture mechanics. Apparent K_{Ith} which is calculated from external applied stress and crack length would increase with the ρ at the crack tip. This agrees with the result that the K_{Ith} value for 1.30CT of which the ρ at a crack tip was greater and crazing stress was smaller than those of the other CT specimens. Thus, it is considered that the ρ at a crack tip, which corresponds to crazing stress σ_c is one of the factors to determine K_{Ith} .

It is considered that the stress which is required to rupture fibrils in crack tip craze (craze fibril rupture stress, σ_d) is also one of the factors. In creep test, creep specimens fractured under creep rupture stresses. Suppose that the creep specimens fracture when the creep rupture stresses are applied to fibrils in crazes on the creep specimens, it is considered that creep rupture stress is just as much as σ_d . σ_d for each specimen was defined as creep rupture stress in 100 s, in this discussion.

When a stress is applied to crack tip craze, K_{Ith} will increase with σ_d . As shown in Table II, creep rupture stress decreases with an increase in sorbed water in creep test specimens. This shows that K_{Ith} should decrease with an increase in sorbed water, if K_{Ith} increases with σ_d . However, the K_{Ith} value for 1.30CT, in which the amount of sorbed water is the most of CT specimens tested, may depend on the balance among ρ at a crack tip, crazing stress and σ_d .

Therefore, we attempt to calculate K_{Ith} from ρ at the crack tip, σ_c and σ_d and to compare measured K_{Ith} quantitatively for each CT specimen.

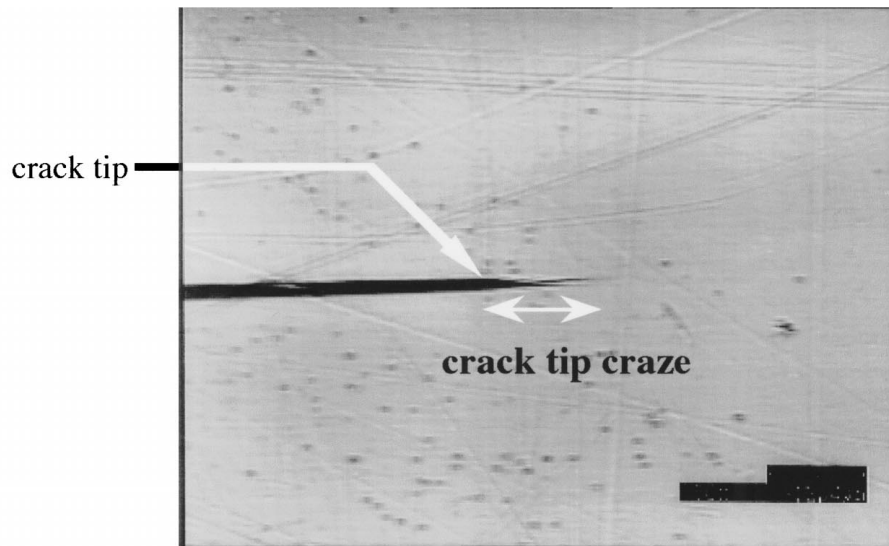
The origin of coordinate axes was defined as a crack tip on the surface of a CT specimen. When an external load is applied to elastic body which contains crack, the $(\sigma_y)_{max}$, which is the stress in the y direction at the craze tip, is given by Creager *et al.* [18]. When stress in the y direction, $\sigma_y(x)$, from $(x, y) = (0, 0)$ to $(x, y) = (x_1, 0)$ distributes as shown in Fig. 11a, it can be approximated by:

$$\sigma_y(x) = \frac{a K_I}{\sqrt{2\pi(x+b)}} \quad (5)$$

where K_I is stress intensity factor, and a and b are constants which can be calculated from $\sigma_y(x=0) = (\sigma_y)_{max}$ and $\sigma_y(x=x_1) = \sigma_1$ at a given K_I . If x_1 and σ_1 are given, the a and b can be calculated. If $\sigma_y(x)$ is equally distributed from $(x, y) = (0, 0)$ to $(x, y) = (x_1, 0)$, for example the region from $x = 0$ to $x = x_1$ plastically deforms as shown in Fig. 11b, the equally distributed stress, $(\sigma_y)_{ave}$ is:

$$(\sigma_y)_{ave} = \frac{1}{x_1} \int_0^{x_1} \sigma_y(x) dx \quad (6)$$

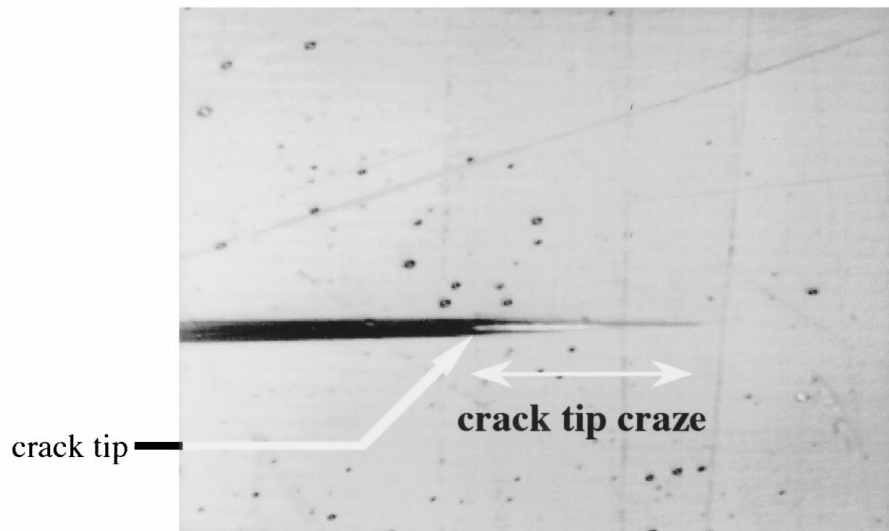
Suppose that the stress applied to craze fibrils near the crack tip is uniform, Equation 6 can be applied to



crack tip craze
length $10\mu\text{m}$
width $1\mu\text{m}$

(a) 0.05CT

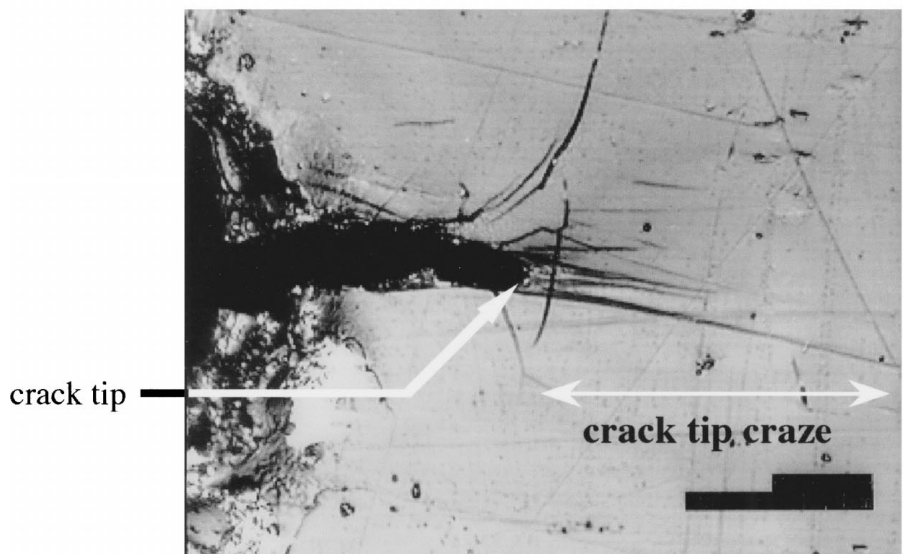
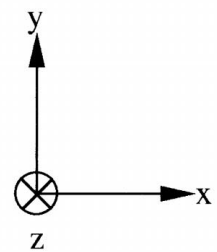
$10\mu\text{m}$



crack tip craze
length $12\mu\text{m}$
width $2\mu\text{m}$

(b) 0.40CT

$10\mu\text{m}$



crack tip craze
length $100\mu\text{m}$
width $10\mu\text{m}$

(c) 1.30CT

$30\mu\text{m}$



crack propagation
direction

Figure 10 Micrographs of crack tips of 0.05CT, 0.40CT and 1.30CT under K_I of $0.8\text{ MPa}\sqrt{\text{m}}$.

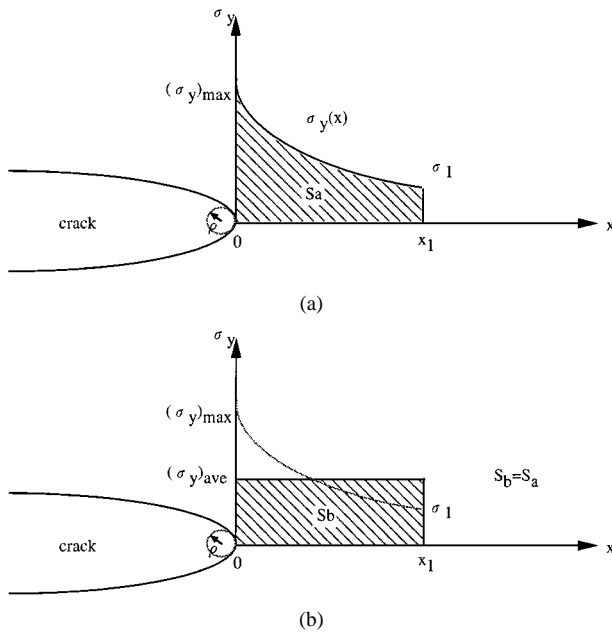


Figure 11 Stress distribution from a crack tip to $x = x_1$. The radius of curvature at the crack tip is ρ . (a) elastic body (b) body plastically deformed from the crack tip to $x = x_1$.

the stress field in a single craze at a crack tip. Then σ_1 can be replaced with σ_c . The craze length near the crack tip and ρ at the crack tip in each CT specimen as shown in Fig. 10a–c is nearly as much as average craze length and a half of the craze width of each creep specimen, respectively, under a K_I of 0.8 MPa \sqrt{m} as shown in Table II. Since craze width at the crack tip in a PMMA specimen under static loading is nearly uniform [4] and craze width and craze length is in a one to one correspondence as shown in Fig. 7, average craze length and a half of the craze width of each creep specimen as shown in Table II were substituted for x_1 , and the ρ . If the crack starts to propagate when $(\sigma_y)_{ave}$ reaches σ_d under $K_{Ith,cal}$, $K_{Ith,cal}$ is:

$$K_{Ith,cal} = \frac{l\sigma_d}{\int_0^l \sigma_y(x) dx} \quad (7)$$

where l is craze length at the crack tip.

The calculated results of $K_{Ith,cal}$ for each sample is shown in Table III. $K_{Ith,cal}$ for each CT specimen agrees well with the experimental value. It is considered that the assumption that the ρ at the crack tip, crazing stress and σ_d control K_{Ith} is approximately plausible. Thus, crack tip blunting and long craze strongly raise crack propagation threshold even though σ_c and σ_d are comparatively small. It is considered that the reduction of stress concentration at the crack tip due to crack tip

blunting and long craze is a cause of the highest K_{Ith} value for 1.30CT. However, $K_{Ith,cal}$ for 1.30CT is approximately 20 percents smaller than the K_{Ith} value. It can be observed in Fig. 10 that some crazes appear near the crack tip in 1.30CT. It is considered that the net σ_y at the crack tip may be smaller than the $(\sigma_y)_{ave}$ which is obtained from the assumption of a single craze at a crack tip.

4.2. Effects of sorbed water on the slope of CPS curve

For 1.30CR, a craze can grow 100 μm in length under a stress of 50 MPa in approximately 20 s, however, the creep rupture stress was below 1.1 times as high as the crazing stress. Once the crack in 1.30CT propagates, the crack tip becomes sharp, and the stress near the crack tip can easily reach σ_d , and the crack unstably propagates. If crack propagation rate is higher than the growth rate of a crack tip craze and the crack tip catches up with the craze tip, the specimen may unstably fracture without plastic deformation. It is considered that this may be a cause of fracture in an extremely short time for 1.30CT.

For samples containing 0.40 wt% water, the creep rupture stress was more than 1.2 times as much as the crazing stress, and craze geometry resembles each other, however, the slope of the CPS curve for 0.40CT was much steeper than that for 0.05CT. This shows that the difference in the slopes of these CPS curves cannot be well explained only from the results of the creep tests.

Therefore, the fracture surfaces of 0.05CT and 0.40CT were observed in order to understand the effects of sorbed water on the slopes of the CPS curves. Fig. 12 shows the fracture surfaces for 0.05CT and 0.40CT. The fracture surface for 0.05CT is covered with some black or gray zones, and these zones are parallel to the x direction, while that for 0.40CT is comparatively flat at low crack propagation rate ($<7 \times 10^{-7}$ m/s). These suggest that crack propagation mechanisms differ between 0.05CT and 0.40CT.

The fracture surface of 0.05CT consists of flat regions and ledge regions (Fig. 13a and b). The former regions are indicated as gray zones in the micrograph, while the latter regions are indicated as black zones. When white light reached a flat region, the reflective light from the region was seen colorfully with using an optical microscope, while the ledge regions were still black, and thus there was no reflective light from this region. This shows that flat regions result from craze-controlled crack propagation [19]. Furthermore, the difference in

TABLE III Comparison between calculated K_{Ith} ($K_{Ith,cal}$) and experimental K_{Ith} . Craze length and craze width are from the results of creep test. Crazing stress is the stress at which crazes appear in 100 sec, and stress to draw out fibrils is the stress at which creep specimens rupture in 100 sec

designation of CT specimen (creep specimen)	craze length $l/\mu\text{m}$	craze width $w/\mu\text{m}$	crazing stress/MPa	stress to draw out fibrils/MPa	$K_{Ith,cal}/\text{MPa}\sqrt{m}$	$K_{Ith}/\text{MPa}\sqrt{m}$
0.05CT(0.05CR)	10	2.7	56	66	0.82	0.88
0.40CT(0.40CR)	10	2.7	50	62	0.82	0.86
1.30CT(1.30CR)	100	5.6	46	50	1.01	1.2

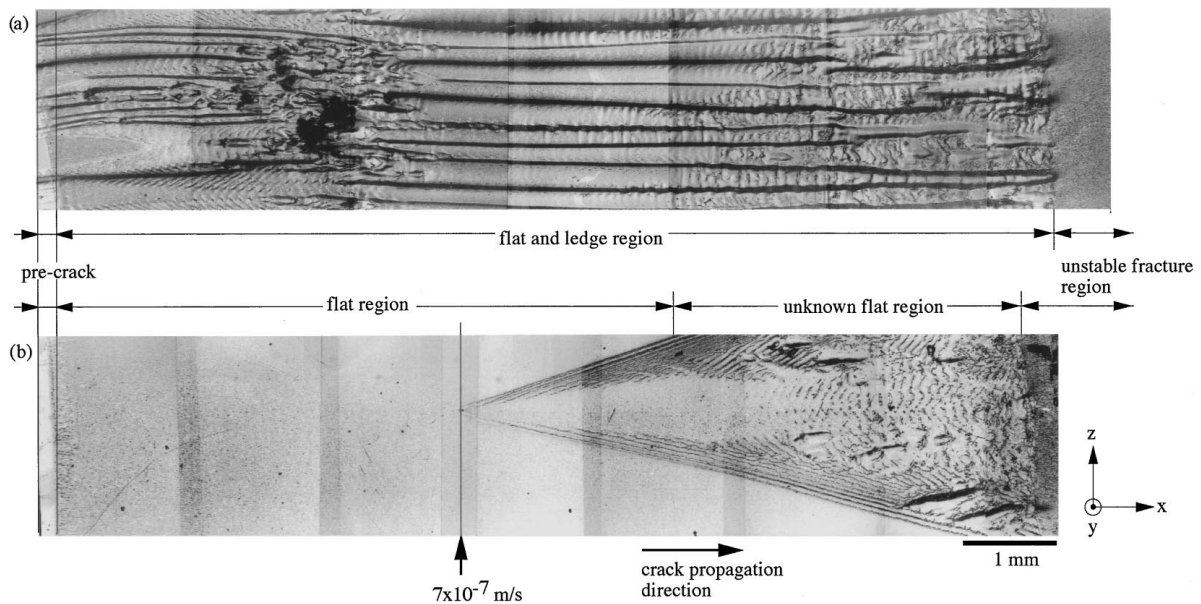


Figure 12 Fracture surfaces of CT specimens carried out CPS tests. (a) 0.05CT (b) 0.40CT.

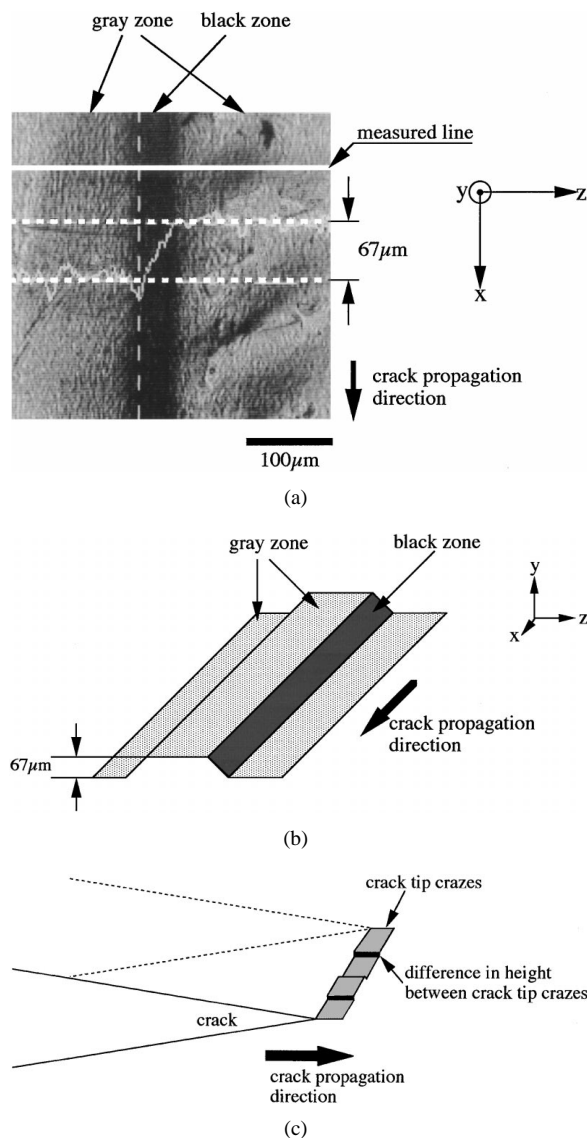


Figure 13 (a) Difference in height between gray zones of flat and ledge region on the fracture surface of 0.05CT under a K_I of $0.95 \text{ MPa}\sqrt{\text{m}}$. (b) A schematic three-dimensional view of the fracture surface. (c) Schematic three-dimensional views near crack tip. A gray zone consists of a crack tip craze. The crack propagates through crack tip crazes.

height between a flat region and a neighboring flat region is more than $50 \mu\text{m}$. If the crack in 0.05CT propagates through a single craze ahead of the crack tip, the difference in height cannot be explained, because the craze width is less than $10 \mu\text{m}$. Thus a flat region is due to crack propagation through a craze, and the height in the y direction among the crazes differ each other. The ledge regions may result from crack propagation without crazing such as shear-controlled crack propagation. A schematic three-dimensional figure is shown in Fig. 13c. The shear yielding stress for PMMA is greater than the crazing stress [20]. This implies that the formation of ledge regions may be a cause of a decrease in crack propagation rate. This idea is plausible also from experimental results that crack propagation rate under craze-controlled mechanisms for polystyrene-carbonate is higher than that under shear-controlled mechanisms [21].

For 0.40CT, the roughness of the flat region of fracture surface is less than $10 \mu\text{m}$ (Fig. 14a), and the reflective light with using an optical microscope was colorfully observed on the region. This shows that this flat region results from crack propagation through a single craze at the crack tip [19]. The schematic three-dimensional figure for this type of crack propagation is shown in Fig. 14b. It has been reported that a craze ahead of crack tip is an easy path for crack propagation and this leads to a relatively high crack propagation rate [21]. It is considered that a cause for the steeper slope of CPS curve for 0.40CT than for 0.05CT, may be crack propagation through a crack tip craze.

In creep test, sorbed water in 0.40CR acted as a plasticizer which caused to increase a number of crazes as shown in Table II, however, the crack tip craze in 0.40CT was a single craze which spreads all over the crack front as shown in Fig. 14. It is considered that sorbed water in 0.40CT may also act as a plasticizer which causes to lengthen the craze in the x direction in the local region near the crack tip at which stress concentrated.

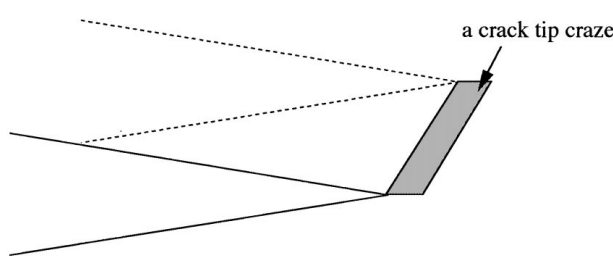
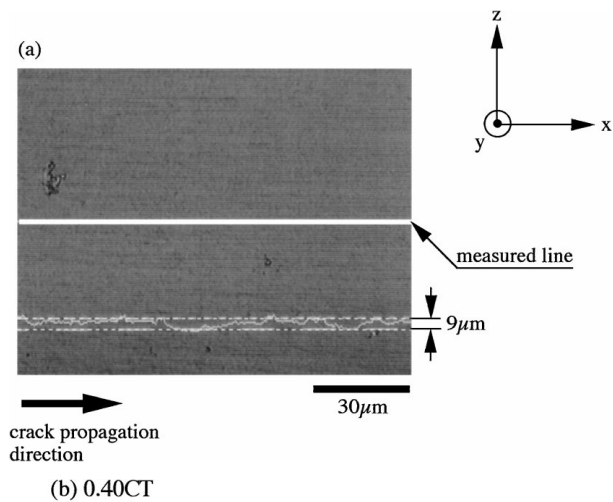


Figure 14 (a) Flat region of the fracture surface of 0.40CT under a K_I of $0.87 \text{ MPa}\sqrt{\text{m}}$. The roughness is much smaller than that of flat and ledge region in fracture surface of 0.05CT. (b) A schematic three-dimensional view ahead of the crack tip. The crack propagates through a crack tip craze.

It can be observed in Fig. 12 that, following the flat region on the fracture surface for 0.40CT, another region appears at a crack propagation rate of $7 \times 10^{-7} \text{ m/s}$ and spreads out with crack propagation. However, the changes in the slope of the CPS curve before and after the appearance of the region on the fracture surface is

scarcely seen. The reflective light on a large extent of the region with using an optical microscope was seen colorfully, and the difference in height between the region and the flat region is $50 \mu\text{m}$ to $100 \mu\text{m}$ (Fig. 15). This suggests that the region may be resulted from the crack propagation mechanisms which is different from the mechanism through the craze in the flat region, however, the formed mechanisms has not been clarified yet.

5. Conclusions

We investigated the effects of sorbed water on crack propagation behavior in PMMA under static tensile loading. The detailed results obtained are as follows:

1. K_{Ith} for samples containing more than 0.40 wt% water increased with the amount of sorbed water. K_{Ith} for samples containing less than 0.40 wt% water scarcely changed with the amount of sorbed water. The reduction of stress concentration near a crack tip due to a long and wide crazing region near the crack tip is a cause of high K_{Ith} value for specimens containing high amount of sorbed water, though the crazing stress and creep rupture stress for the specimens were lower than those for other specimens. Comparatively high stress concentration near a crack tip due to a short and narrow craze near the crack tip is a cause of low K_{Ith} value for specimens containing low amount of sorbed water, though the crazing stress and creep rupture stress for the specimens were higher than those for other specimens.

2. Slopes of CPS curves increased with amount of sorbed water. The gentle slope for samples containing low amount of sorbed water may result from shear-controlled crack propagation mechanisms. The steep slope for samples containing more than 0.40 wt% water may result from a lack of the mechanisms.

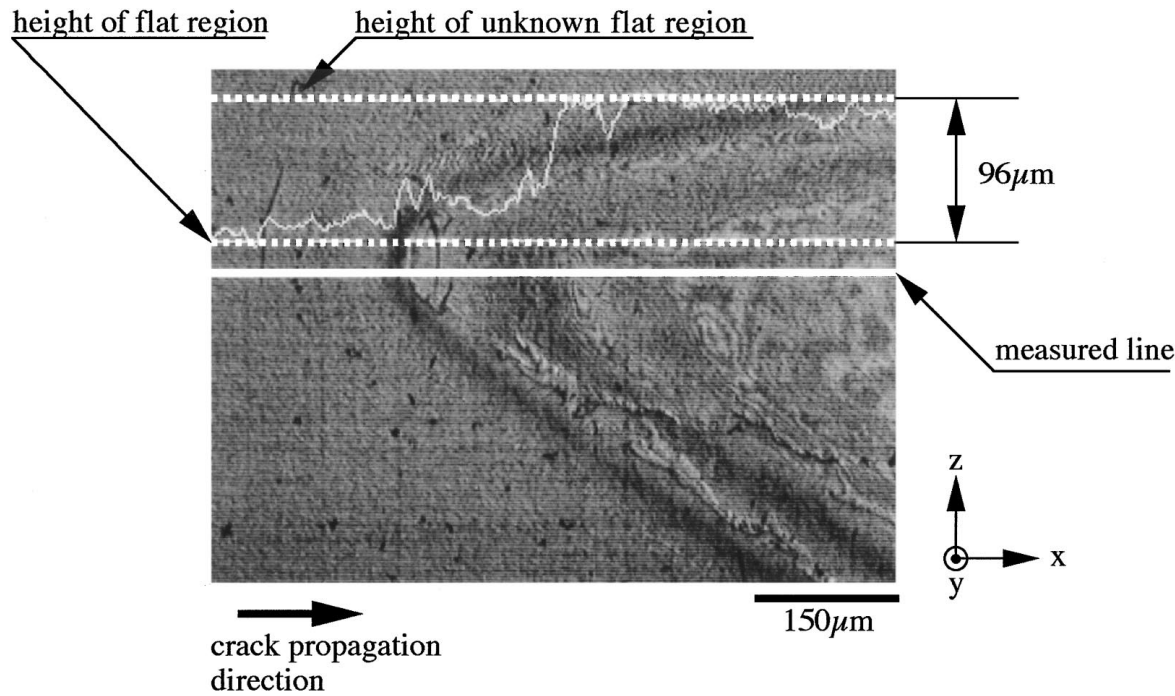


Figure 15 Micrograph near transition region from flat region to another region of the fracture surface of 0.40CT. The roughness between both regions is $96 \mu\text{m}$. The latter region is seemed nearly flat.

Acknowledgements

Cast PMMA sheets were supplied by Mitsubishi Rayon Co., Ltd, Japan.

References

1. R. P. KAMBOUR, *J. Polym. Sci. (A)* **3** (1965) 1713.
2. M. I. BESSENOV and E. V. KURSHINSKII, *Sov. Phys.-Solid State* **3** (1961) 1957.
3. H. R. BROWN and I. M. WARD, *Polymer* **24** (1983) 1213.
4. W. DOLL, L. KONCZOL and M. G. SCHINKER, *ibid.* **24** (1983) 1213.
5. L. KOENCZOEL and K. SEHANOBISH, *J. Macromol. Sci. Phys.* **B26**(3) (1987) 307.
6. M. BEVIS and D. HULL, *J. Mater. Sci.* **5** (1970) 983.
7. M. BOTSIS, A. CHUDNOVSKY and A. MOET, "Micromechanisms of Crack Layer Propagation in Polystyrene Under Cyclic Loads" (XXXIX ANTEC-SPE, Chicago, 1983) p. 444.
8. A. CHUDNOVSKY, A. MOET, R. J. BANKERT and M. T. TAKEMORI, *J. Appl. Phys.* **54** (1983) 5567.
9. M. T. TAKEMORI and R. P. KAMBOUR, *J. Mater. Sci.* **16** (1981) 1110.
10. N. J. MILLS and N. J. WALKER, *ibid.* **15** (1980) 1840.
11. H.-S. KIM, Y.-W. MAI and B. COTTERELL, *Polymer* **29** (1988) 277.
12. A. H. ANDREWS and S. P. BARNES, "Deformation, Yield and Fracture of Polymers" (Plastics and Rubber Institute, Cambridge, 1982) p. 8.1.
13. Y. IMAI and N. BROWN, *J. Mater. Sci.* **11** (1976) 417.
14. P. TRASSAERT and R. SHIRNER, *ibid.* **18** (1983) 3004.
15. L. S. A. SMITH and J. A. SAUER, *Plastics and Rubber Processing and Applications* **6** (1986) 57.
16. L. JOSSELAND, R. SCHIRNER and P. DAVIS, *J. Mater. Sci.* **30** (1995) 1772.
17. W. DOLL, "Advances in Polymer Science, 52/53" (Springer-Verlag, Berlin, Heidelberg, 1983) p. 105.
18. M. CREAGER and P. S. PARIS, *Int. J. Fract. Mech.* **3** (1967) 247.
19. M. HIGUCHI, *Repts. Res. Inst. Appl. Mech. Kyushu Univ.* **6** (1958) 173.
20. S. S. STERNSTEIN and L. ONGCHIN, *Polymer Preprints, Am. Chem. Soc., Div. Polymer Chem.* **10**(2) (1969) 1117.
21. M. T. TAKEMORI, *Polym. Eng. Sci.* **27** (1987) 46.

Received 26 August 1998
and accepted 28 March 2000